Response to the reviews of TC-2018-108 "The potential of sea ice leads as a predictor for seasonal Arctic sea ice extent prediction" by Yuanyuan Zhang, Xiao Cheng, Jiping Liu, and Fengming Hui

We greatly appreciate the thoughtful comments from the reviewers. According to the reviewer's comments, we revised the original manuscript.

Responses to reviewer #1 comments

Thank you very much for your careful reviewing of our manuscript. All issues raised have been considered thoroughly. The point-to-point response to the issues is appended below.

General comments:

Question 1a) *MODIS infrared observations of the surface are only available under cloud-free conditions. Therefore, it is potentially misleading to directly calculate the pan-Arctic or regional area of sea-ice leads from the gridded observational product as done by the authors. A brief look at one season of daily gridded maps of the sea-ice lead data product reveals that a large fraction of the sea-ice covered area is obscured by clouds for almost every day, and as expected there are large day-to-day variations in the cloud cover. Therefore, it is not clear at all how SILA as calculated by the authors relates to the area of actually present sea-ice leads. What if the year-to-year variability of SILA shown in Figure 2a is actually dominated by the variability in cloud cover obscuring a constant actual lead area to varying degrees? Varying cloud cover would be an alternative explanation for varying summer ice extent, because winter-time clouds keep the surface warm and inhibit sea-ice growth. The role of clouds needs to be properly discussed before a robust conclusion about the lead area can be drawn.*

Question 1b) *It is also evident from the gridded maps of the sea-ice lead product that polynyas and the marginal ice zone in the Atlantic sector are wrongly classified as leads. It might well be that year-to-year variability in the area of polynyas and the width of the marginal ice zone in the Atlantic sector is responsible for the year-to-year variability in the SILA calculated by the authors. This would then invalidate their main conclusion as it is specific to sea-ice leads. Please provide some further analysis that quantifies how much of the SILA signal comes from polynyas and the Atlantic marginal ice zone.*

Question 2) *Related to point (1) above, it would make the author's main conclusions more credible if they were supported by independent observational data, modelling results, or process studies. I would leave it up to the authors to decide what is most appropriate. An idea would be to have a look at observational products of cloud cover on the one hand, and an observational product of winds and sea-ice drift on the other hand. The first is important for thermodynamic ice growth, the second for the creation of leads. From studying the inter-annual variability of clouds, sea-ice drift and winds, some sup- port or additional doubt could be derived regarding the author's main conclusions.*

Response:

We appreciate reviewer's suggestions. Since question 1a, 1b and 2 are related, here we address them together.

1) We agree with the reviewer that cloud contamination is a major issue plaguing the retrieval of the pan-Arctic sea ice leads from the MODIS infrared observation. To address this issue, Willmes and Heinemann (2015a) used multi-temporal satellite images that make full use of cloud-free pixels and assumed that changes of surface characteristics are insignificantly over synoptic time scale for detecting sea ice leads in pixels obscured by clouds. The probability of a clear-sky view within a day is increased associated with the convergence of satellite tracks in high latitudes. As shown in Willmes and Heinemann (2015b), on average, the Arctic has a clear-sky frequency of 30-60% in the daily aggregates. The lowest availability of clear-sky data is in the Chukchi Sea (see Figure 3 in Willmes and Heinemann, 2015b for details). To further mitigate the issue of cloud contamination, William and Heinemann (2015a, b) implemented a fuzzy cloud artifact filter that employs temporal and spatial object characteristics to distinguish between physical sea ice leads and artifacts that arise from clouds.

References:

Willmes, S. and Heinemann, G.: Pan-Arctic lead detection from MODIS thermal infrared imagery, Annals of Glaciology, 56, 29-37, 2015a.

Willmes, S. and Heinemann, G.: Sea-ice wintertime lead frequencies and regional characteristics in the Arctic, 2003–2015, Remote Sensing, 8, 4, 2015b.

2) To further address the reviewer's concern, we compared the MODIS sea ice leads data used in this study with the Synthetic Aperture Radar (SAR) images under cloudy conditions. Compared to MODIS that receives thermal emissions or reflected components, SAR allows for penetration through most clouds and precipitation. We calculated backscatter coefficients from the Sentinel-1A Extra-Wide swath HH polarization images using the Sentinel Application Platform and projected them on the NSIDC polar-stereographic grid with a spatial resolution of 100 m. Cloudy conditions are determined using the MOD08 Level3 daily cloud fraction product (Hubanks et al., 2018). For example, Figure 1 and 2 show the MODIS cloud fraction, SAR backscatter coefficient image, and MODIS sea ice leads in the northern Beaufort Sea on April 11, 2015 and the central Arctic Ocean that is northeast of Greenland on April 9, 2015, respectively. Compared to SAR images, the MODIS sea ice leads data can capture the correct spatial distribution of sea ice leads under cloudy conditions. The consistence between the MODIS sea ice leads data and SAR images gives us more confidence about this data. Thus, the sea ice lead area (SILA) calculated in this study is related to the area of actually present sea ice leads.

Reference:

Hubanks, P., Platnick, S., King, M., and Ridgway, B.: MODIS atmosphere L3 gridded product algorithm theoretical basis document ATBD & Users Guide Reference Number: ATBD-MOD-30, Collection 006, Version 4.3, 128, 2018.

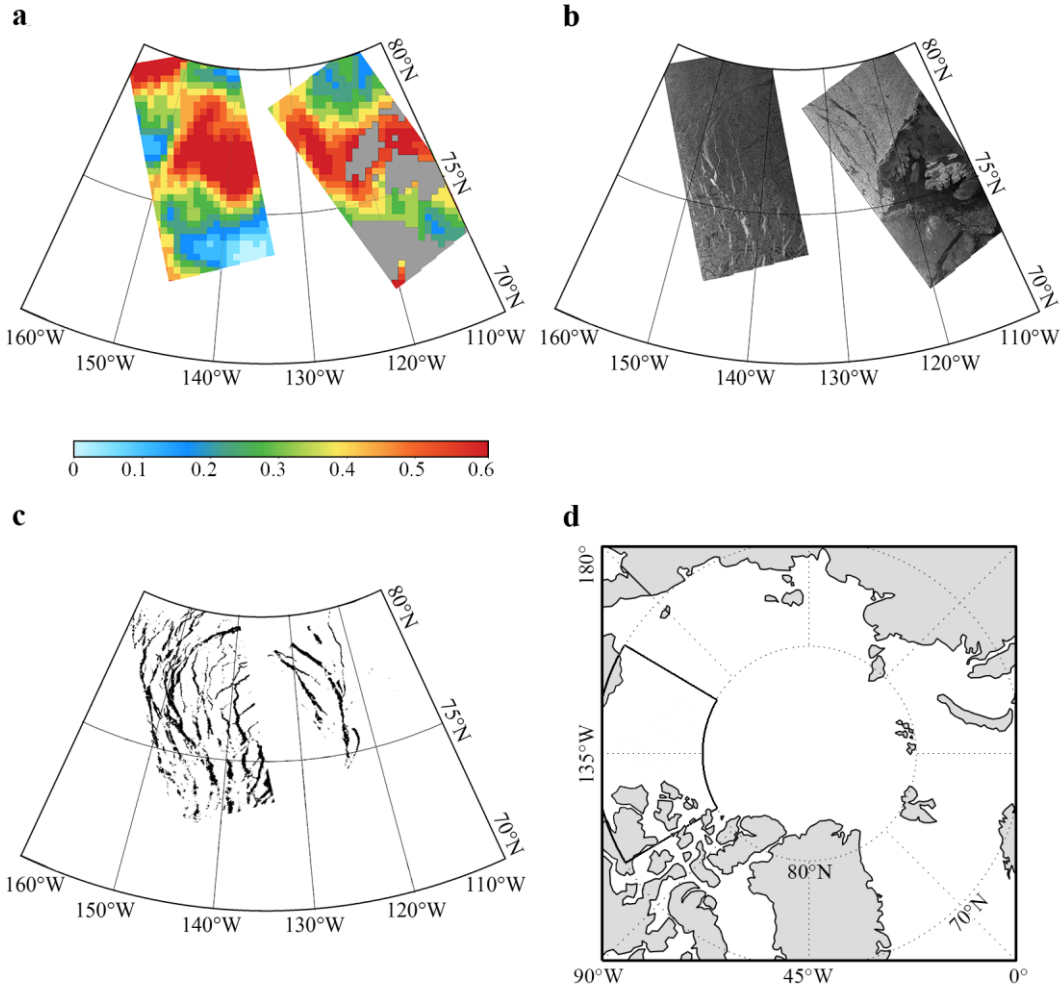

Figure 1. (a) MODIS cloud fraction (%), (b) SAR backscatter coefficient image, and (c) MODIS sea ice leads in the highlighted area (the northern Beaufort Sea) as shown by the box in (d) on April 11, 2015.

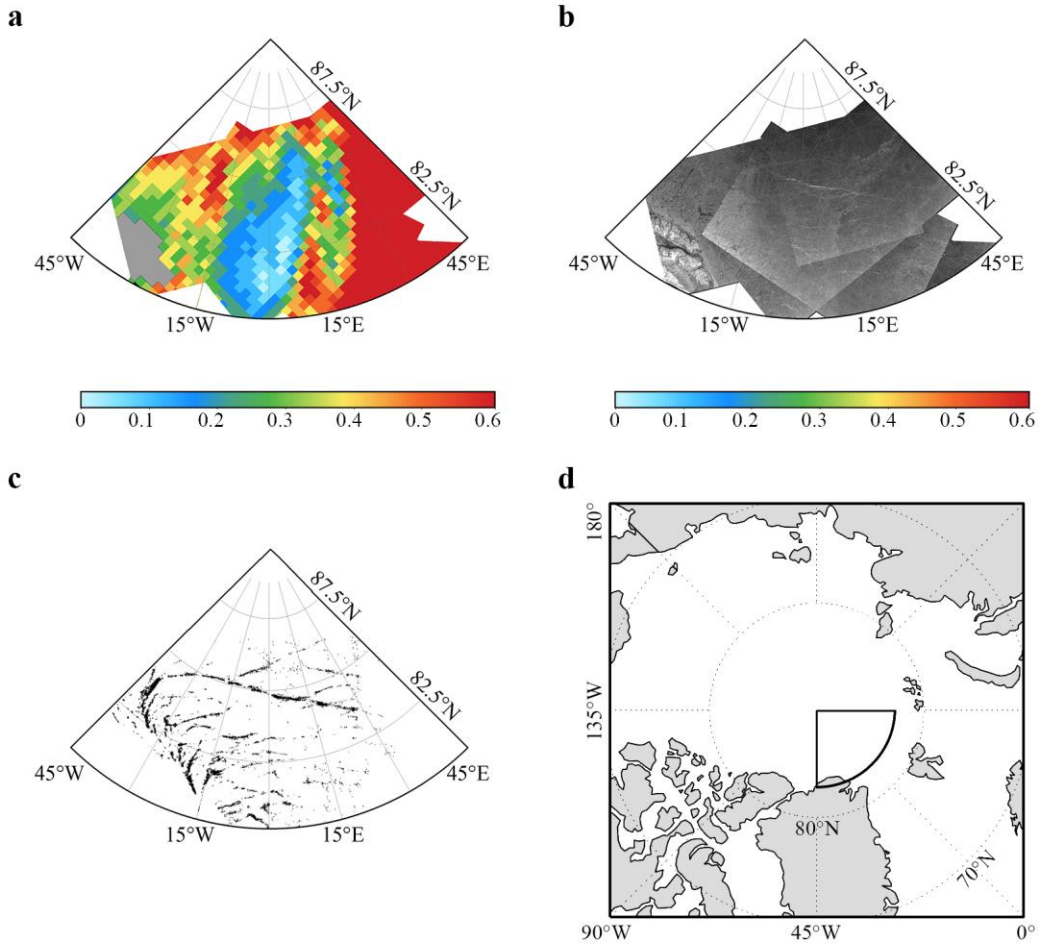

Figure 2. (a) MODIS cloud fraction (%), (b) SAR backscatter coefficient image, and (c) MODIS sea ice leads in the highlighted area (the central Arctic Ocean that is northeast of Greenland) as shown by the box in (d) on April 9, 2015.

3) More importantly, we examined the relationship between the area of clouds in the Arctic Ocean from late winter to mid-spring and Arctic sea ice extent during the melting season. Following the same procedure applied to the calculation of sea ice leads in the manuscript, the area of clouds is defined as the sum of the product of the cloud fraction and the area of the grid box (625 km^2) using the MOD08 daily cloud fraction data projected on the NSIDC polar-stereographic grid (25km). We then calculated correlation coefficients between the de-trended time series of the integrated the area of clouds at each grid point and the de-trended time series of the total sea ice extent in July. Figure 3 shows significant correlations that exceed the 95% confidence level. It appears that the region having significant correlations associated with the cloud area is very different from that of sea ice leads, and the overlapped significant correlations only occurs in a small area as shown by grey crosses in Figure 3. We further calculated the correlation between time series of the area of clouds integrated to the day given and time series of July Arctic sea ice extent. Note that time series of the area of clouds is calculated over the region where sea ice leads and extent have significant correlations

except the overlapped area (orange color in Figure 3). As shown in Figure 4, there is no significant correlation between the cloud area and July sea ice extent throughout the entire period. By contrast, significant correlation between the area of sea ice leads and July sea ice extent first occurs in mid-to-late February, the magnitude of the correlation gradually increases and the strongest relationship is achieved as the integration extended to early April (see Figure 4 in the original manuscript). This suggests that the significant relationship between the area of sea ice leads and July sea ice extent is related to the area of actually present sea ice leads, rather than cloud cover.

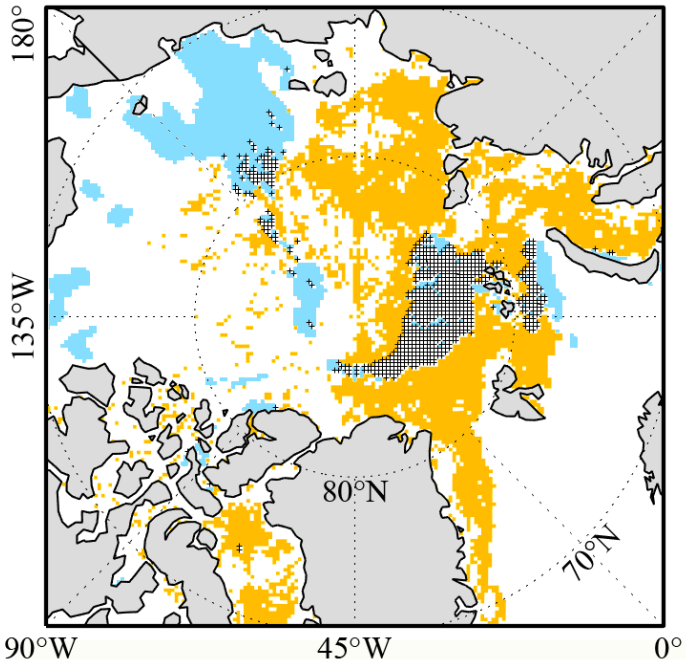

Figure 3. Spatial distribution of significant correlations between the area of clouds (blue) and sea ice leads (orange) integrated from 1 January to 30 April with July sea ice extent. Grey cross denotes the overlapped significant correlations.

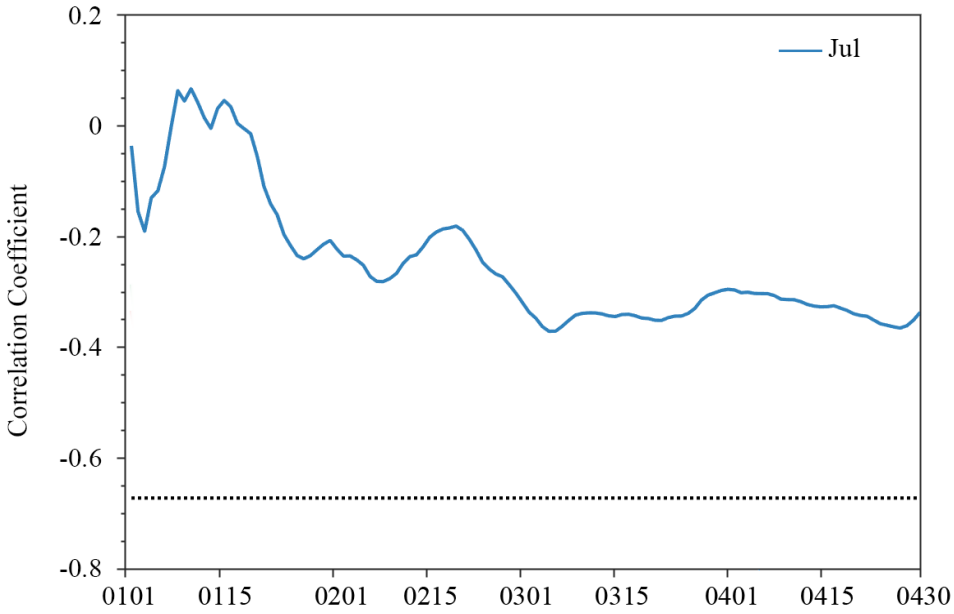

Figure 4. Evolution of correlation coefficients between the total area of cloud integrated from January 1 to April 30 and the total Arctic sea ice extent in July (blue line) during 2003-2015. The horizontal line is 99% (black dot) confidence level.

4) As suggested by the reviewer, open water/polynyas in the marginal ice zone can be wrongly classified as sea ice leads. Although the retrieval method of Willmes and Heinemann (2015a) is based on significant positive surface temperature anomalies associated with the presence of a lead with respect to its surrounding area, they removed swath-level temperature gradients by deriving the local temperature anomalies based on the temperature distribution in 51 x 51 kernel. This tends to reduce the misclassification of leads and open water/polynyas. Their data is limited to January to April because their method relies on a pronounced thermal contrast between leads and open water/polynyas. For example, Figure 5 shows the MODIS sea ice leads fraction and open water fraction computed from the NASA Team sea ice concentration data (25 km) on April 30, 2015. To make the two data comparable, the 1.5 km MODIS sea ice leads data is projected on the NSIDC polar-stereographic grid with a spatial resolution of 25 km. Clearly, sea ice leads fraction in the marginal ice zone in the Chukchi and Beaufort Seas (Figure 5b) and the Greenland, Iceland and Norwegian (GIN) Seas (Figure 5d) is different from that of open water, (Figure 5a and c), and the magnitude of sea ice leads fraction is much smaller than that of open water.

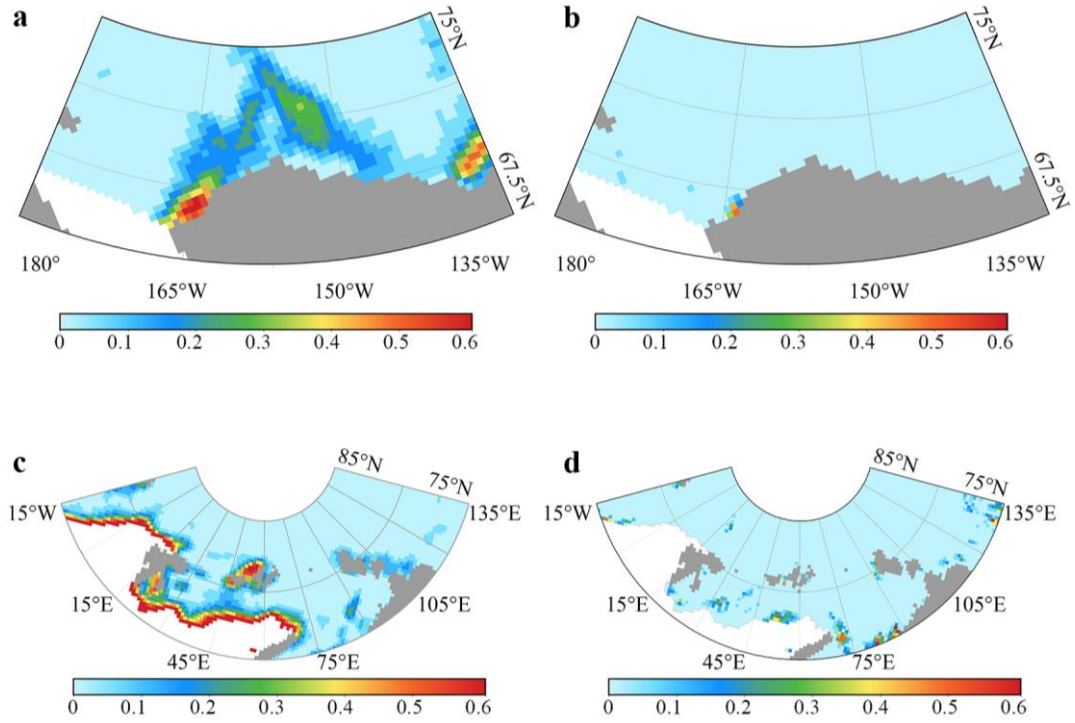

Figure 5. Spatial distribution of open water fraction (left column) and sea ice leads fraction (right column) in the marginal ice zone in the Chukchi and Beaufort Seas and the GIN Seas on April 30, 2015.

5) To further address the reviewer's concern, we examined the relationship between the area of open water calculated from NASA Team sea ice concentration data in the Arctic Ocean from late winter to mid-spring and Arctic sea ice extent during the melting season. Following the same procedure applied to the calculation of sea ice leads in the manuscript and clouds above, the area of open water is defined as the sum of the product of the open water fraction and the area of the grid box (625 km^2). We then calculated correlation coefficients between the de-trended time series of the integrated the area of open water at each grid points and the de-trended time series of the total sea ice extent in July. Figure 6 shows significant correlations that exceed the 95% confidence level. It appears that scattered areas have significant correlations associated with the open water area, and the overlapped significant correlation only occurs in a small area as grey crosses in Figure 6. We further calculated the correlation between time series of the area of open water integrated to the day given and time series of July Arctic sea ice extent. Note that time series of the area of open water is calculated over the regions where sea ice leads and sea ice extent have significant correlations except overlapped area (orange color in Figure 6). As shown in Figure 7, there is no significant correlation between the open water area and July sea ice extent. By contrast, significant correlation between the area of sea ice leads and July sea ice extent first occurs in mid-to-late February, the magnitude of the correlation gradually increases and the strongest relationship is achieved as the integration extended to early April (see Figure 4 in the

original manuscript). This suggests that the significant relationship between the area of sea ice leads and July sea ice extent is related to the area of actually present sea ice leads, rather than open water/ polynyas.

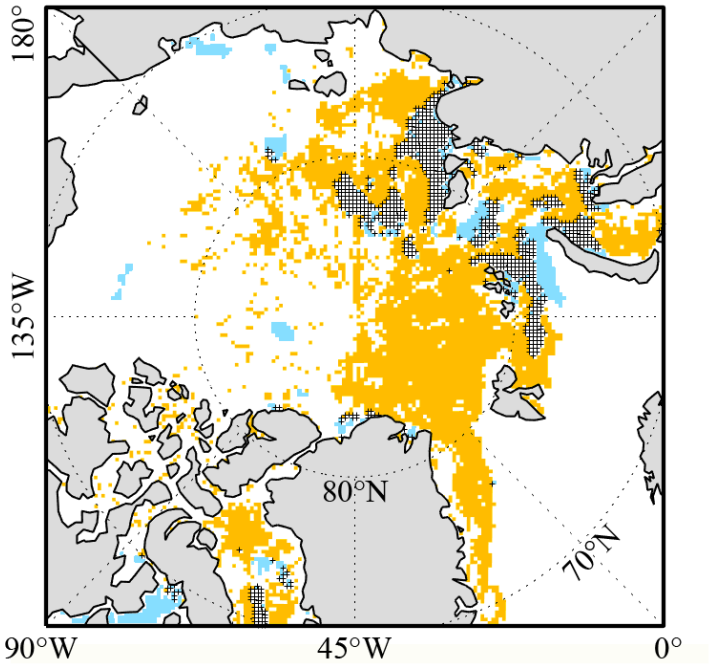

Figure 6. Spatial distribution of significant correlations between the area of open water (blue) and sea ice leads (orange) integrated from 1 January to 30 April with July sea ice extent. Grey cross denotes the overlapped significant correlations.

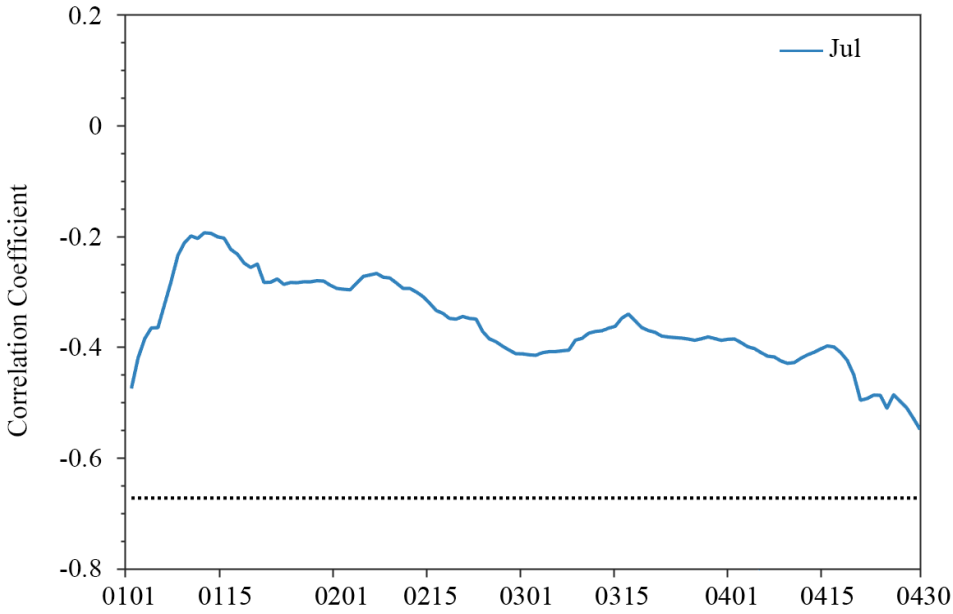

Figure 7. Evolution of correlation coefficients between the total area of open water integrated from January 1 to April 30 and the total Arctic sea ice extent in July (blue line) during 2003-2015. The horizontal line is 99% (black dot) confidence level.

Question 3) *I am a bit sceptical about the skill achieved in "prediction mode" as shown in the right-hand column of Figure 5. For example, the forecasts shown in Figure 5e are almost identical to the regressed values shown in Figure 5a. This is surprising given the moderate amount of correlation in the time series used to construct the linear predictor. Could it be that the authors accidentally used the complete time series to construct the linear predictor, rather than only the first 6 years? Can the authors please check their analysis and provide further evidence that the prediction results in Figures 5e-g have been calculated exactly as described in the text?*

Response:

We double checked our calculation. For the prediction analysis in the original manuscript, we actually used the data from all previous years to determine the slope and intercept of the linear regression model, and then calculated the predicted Arctic sea ice extent anomalies for the years of 2009-2015, instead of only the data of the first six years (2003-2008). For example, the predicted July sea ice extent anomaly in 2009 (2015) is based on the training using the data of 2003-2008 (2003-2014). Here we recalculated the prediction analysis for the years of 2009-2015 by only using the data of the first six years (2003-2008) to determine the slope and intercept of the linear regression model. As shown in Figure 8, the result of the predicted July sea ice extent anomalies (Fig. 8f) is very similar to that in the original manuscript (Fig. 8a), and predictive skill is even slightly better (Fig. 8e and 8j). There is still no predictive skill for August and September sea ice extent.

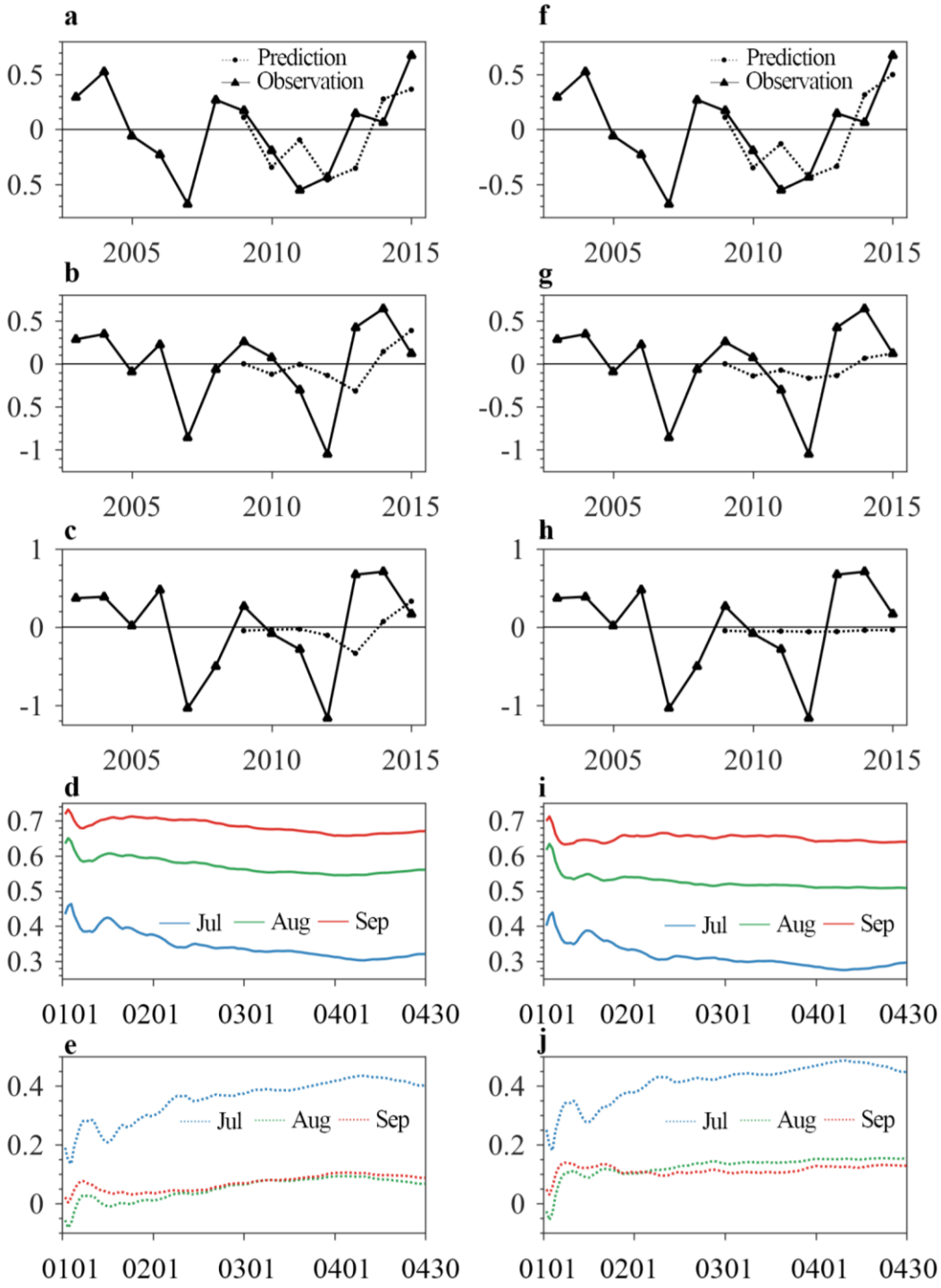

Figure 8. Predicted total Arctic sea ice extent anomalies (million km^2) in (a,f) July, (b,g) August and (c,h) September during 2009-2015 based on the area of sea ice leads integrated from January 1 to April 30, (d,i) the evolution of their prediction errors and (e,j) their forecast skills; Left column: the data of all previous years are used; Right column: only the data from the first six years (2003-2008);The blue, green and red lines are July, August and September, respectively.

Question 4) *The Data Section needs a more detailed description of the MODIS sea-ice leads data set. This description needs to also discuss the limitations and assumptions*

of the data set. This comment is related to points 1a) and 1b) above. Furthermore, I would suggest to rename the section to "Data and Methods" and move lines 9-16 of page 4 to that section. The description of how the SILA is calculated needs to include more details on how clouds and artifacts in the observational data set are treated.

Response:

Based on the reviewer's suggestion, we renamed the section to "Data and Methods", and provided more information about the MODIS sea ice leads data set. We also moved the description of how to calculate the area of sea ice leads (SILA) to this section. Now this section reads as "…In a recent study, Willmes and Heinemann (2015a) presented a non-parameterized global threshold method, which was validated and applied to derive sea ice leads maps from surface temperature anomalies in the Arctic Ocean using the MODIS ice surface temperature product. Daily sea ice leads composites were created. The composite maps indicate the presence of cloud artifacts in the leads identification that arise from ambiguities in the MODIS cloud mask. To mitigate these artifacts, they implemented a fuzzy filter system that employs spatial and temporal object characteristics to distinguish between physical leads and artifacts. This approach advances the potential to retrieve daily leads maps operationally from the MODIS infrared product.

In this study, the pan-Arctic sea ice leads data is obtained from the Data Publisher for Earth & Environment Science (PANGAEA), which is available for the months from January to April for the period 2003-2015 (Willmes and Heinemann, 2015b). The spatial resolution of the daily binary sea ice leads map is about 1.5 km with omission 5% that can reflect sea ice leads variability except the Chukchi Sea (Willmes and Heinemann, 2015a, c), because clear-sky day is less than 15% in the Chukchi Sea. Cloud contamination is a major issue plaguing the retrieval of the pan-Arctic sea ice leads from the MODIS infrared observation. Here we compare the above MODIS sea ice leads data with the Synthetic Aperture Radar (SAR) images under cloudy conditions. Compared to MODIS that receives thermal emissions or reflected components, SAR allows for penetration through most clouds and precipitation. We calculate backscatter coefficients from the Sentinel-1A Extra-Wide swath HH polarization images using the Sentinel Application Platform and project them on the NSIDC polar-stereographic grid with a spatial resolution of 100 m. Cloudy conditions are determined using the MOD08 Level3 daily cloud fraction product (Hubanks et al., 2018). For example, Figure 1 shows the MODIS cloud fraction, SAR backscatter coefficient image, and MODIS sea ice leads in the northern Beaufort Sea on April 11, 2015. Compared to SAR images, the MODIS sea ice leads data can capture the correct spatial distribution of sea ice leads under cloudy conditions. The consistence between the MODIS sea ice leads data and SAR image gives us more confidence about this data.

The Arctic sea ice extent is obtained from the National Snow and Ice Data Center (NSIDC), which is derived from the Nimbus-7 Scanning Multichannel Microwave Radiometer, DMSP Special Sensor Microwave/Imager, and Special Sensor

Microwave Imager and Sounder sensors using NASA Team algorithm(Cavalieri et al., 1996, updated yearly).

The daily total area of sea ice leads is computed from the daily binary sea ice leads map, which is projected on the NSIDC polar-stereographic grid with a spatial resolution of 25 km. During the projection, we calculate the number of pixels with detected sea ice leads in a 25km grid box. Sea ice leads fraction is then defined as the ratio between the number of pixels with detected sea ice leads and the total number of pixels in the 25km grid box. The total area of sea ice leads is the sum of the product of the sea ice leads fraction and the area of the grid box (625 km^2). Here the daily total area of sea ice leads is only calculated when the NSIDC sea ice concentration in the grid box is larger than 15% (commonly used as the threshold to define sea ice edge). ".

References:

Hubanks, P., Platnick, S., King, M., and Ridgway, B.: MODIS atmosphere L3 gridded product algorithm theoretical basis document ATBD & Users Guide Reference Number: ATBD-MOD-30, Collection 006, Version 4.3, 128, 2018.

Willmes, S. and Heinemann, G.: Pan-Arctic lead detection from MODIS thermal infrared imagery, Annals of Glaciology, 56, 29-37, 2015a.

Willmes, S. and Heinemann, G.: Daily pan-Arctic sea-ice lead maps for 2003-2015, with links to maps in NetCDF format, in 30 Supplement to: Willmes, S; Heinemann, G(2105): Sea-Ice Wintertime Lead Frequencies and Regional Characteristics in the Arctic, 2003-2015, Remote Sensing, 8(1),4, doi:10.3390/rs8010004, edited, PANGAEA, 2015b.

Willmes, S. and Heinemann, G.: Sea-ice wintertime lead frequencies and regional characteristics in the Arctic, 2003–2015, Remote Sensing, 8, 4, 2015c.

Specific comments

1) In the title, the last word "prediction" is a duplication of "predictor" and needs to be removed. "seasonal" should be replaced by "summer", because only the months July-September are considered.

Response:

We changed the title to "The potential of sea ice leads as a predictor for summer Arctic sea ice extent" and this issue has been checked throughout the manuscript.

2) In the abstract, line 14, the wording "accurately predicted" is subjective and ambiguous. Please provide numbers.

Response:

The sentence is changed to "Our results show that July pan-Arctic sea ice extent can be predicted from the area of sea ice leads integrated from mid-winter to late spring with the prediction error of 0.28 million km^2 that is smaller than the standard deviation of the observed interannual variability.".

3) The quantity defined on page 7 is not a forecast skill, but rather a potential forecast skill. A forecast skill (score) is always based on comparing the skill of the forecast with the skill of a reference forecast (e.g. climatology, or a linear trend forecast). I would suggest that in this case comparison with a linear-trend would be appropriate, e.g. S=1-RMSE(SILA regression)/RMSE(trend). See Jollife and Stephenson (2012) for an introduction into forecast verification.

Response:

Based on the reviewer's suggestion, we recalculated the forecast skill using the following equation:

$$S = 1 - \frac{\sigma_f}{\sigma_r}$$

where σ_f is the RMSE of the prediction error and σ_r is the RMSE of the observed July, August and September sea ice extent anomalies (with trend), respectively(0.54, 0.60 and 0.73 million km^2 during 2003-2015), respectively. As shown in Figure 9b, the evolution of forecast skills based on the reviewer's suggestion (S=1-RMSE(SILA regression)/RMSE(trend)) is similar to that of Figure 5i in the original manuscript (that is for July sea ice extent prediction, the predictive skill gradually increases with lengthening integration period and becomes the highest in late April). Again, there is no predictive skill for August and September sea ice extent.

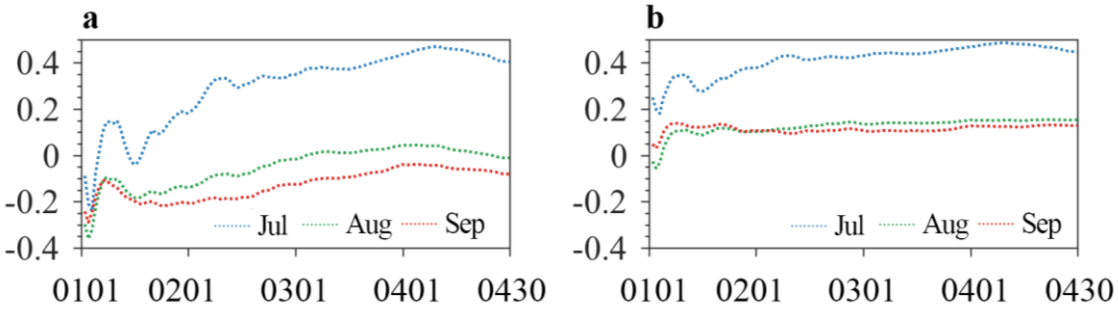

Figure 9. The evolution of forecast skills based on the integrated area of sea ice leads starting from January 1, (a) S=1-MSE(SILA regression)/MSE(detrend), (b) S=1-RMSE(SILA regression)/RMSE(trend). The blue, green and red dot lines are July, August and September, respectively.